Theor Chem Acc (2016) 135:7
DOI 10.1007/s00214-015-1763-y

REGULAR ARTICLE

Dibenzyl disulfide adsorption on Cu(111) surface: a DFT study

Mario Saavedra-Torres[1] · Frederik Tielens[2] · Juan C. Santos[1]

Received: 17 August 2015 / Accepted: 16 November 2015 / Published online: 21 December 2015

Abstract The adsorption of dibenzyl disulfide (DBDS) on a Cu(111) surface model was investigated by using density functional calculations, considering energetic and electronic aspects. Several complexes were generated, where the bridge, hollow hcp, hollow fcc and top adsorption sites were considered. The results show that the Cu–S interaction guides the final complexes, and a secondary π–Cu weak interaction confers an extra stability. The complexes were grouped as physi- or chemisorption according to their adsorption energy applying a distortion decomposition model, with a preference by a double interaction of S with Cu (i.e., hollow hcp and bridge sites). A degree of disulfide bond dissociation was observed in the complexes, being correlated with adsorption energies. From an electronic aspect, it was found that the electronic flow from copper to DBDS occurs in the most stable complexes, checked with charge analysis. These results are in agreement with experimental revelations of copper corrosion on power transformers.

Keywords Copper · Dibenzyl disulfide (DBDS) · DFT · Adsorption

✉ Frederik Tielens
frederik.tielens@upmc.fr

✉ Juan C. Santos
jsantos@unab.cl

[1] Departamento de Ciencias Químicas, Facultad de ciencias exactas, Universidad Andres Bello, Av. República 275, Santiago, Chile

[2] Sorbonne Universités, UPMC Univ Paris 06, CNRS, Collège de France, Laboratoire de Chimie de la Matière Condensée de Paris, 11 Place Marcelin Berthelot, 75231 Paris Cedex 05, France

1 Introduction

The adsorption of sulfur-containing molecules on gold surfaces has attracted much attention, especially since the discovery of the self-assembly of alkyl thiols on Au(111) [1–3]. Thiols adsorption has also been studied on the other coinage metals [4–7]. Thiols [4, 8–15], disulfides [16–19], methionines [20–24], cysteines [25–33], etc., have been studied experimentally and theoretically. The reactivity toward sulfur-containing molecules decreases going down the column of the coinage metals, explaining why molecular adsorption has been successfully observed in the perfectly ordered thiol chains on Au(111) (see reviews on the topic cited higher). On Cu(111), the more reactive surface of the three metals (Cu, Ag and Au), a different picture of the adsorption is expected and observed [5, 34, 35]. The surface itself will reconstruct, and the adsorbed molecules easily dissociated.

Thus, understanding the mechanism of interaction of sulfur-containing molecules is expected to be of high relevance for opening new perspectives toward improving the reactivity or stability of materials used in different applications [36]. Concerning the copper surfaces, sulfur-containing molecules induce copper metal corrosion, which is a chemical phenomenon that triggers serious failures in industrial applications, and especially in power transformers [37, 38].

Dibenzyl disulfide (DBDS) is an additive with antioxidant properties, frequently used in insulating mineral oil employed in power transformers. Under operation conditions, DBDS is known to further copper corrosion in electric equipment, by forming copper (I) sulfide Cu_2S as the main product, with the subsequent production of other sulfur compounds such as benzyl sulfide and dibenzyl sulfide. In spite of successive studies about the chemical

phenomenon, the mechanism remains unclear [39–42]. Since DBDS is related to the commonly used thiol molecules, in the well-known thiol self-assembled monolayers (SAM) on metal surfaces [9, 43–45], the analysis of the metal–sulfur bond is important to complete the already known information on the chemical properties of this type of systems.

In the present paper, the nature of the interaction between Cu(111) and DBDS is theoretically studied. A slab model is used to simulate the copper surface at reasonable accuracy, i.e., using periodic PBE-D2. In particular, we clarify some aspects associated with copper corrosion by DBDS at the DFT level by accounting geometric, energetic and electronic properties that govern the interaction between DBDS and copper. The main focus of attention is to characterize locally the copper–sulfur interaction/bonding.

2 Computational details

2.1 Computational method

Calculations were performed in the frame of periodic DFT by means of the Vienna Ab Initio Simulation Package (VASP 5.3) [46, 47]. The electron–ion interactions were described by the projector augmented wave (PAW) method [48, 49], representing the valence electrons. The convergence of the plane-wave expansion was obtained with a cutoff of 400 eV. The Perdew–Burke–Ernzerhof (PBE) [50, 51] generalized gradient approximation (GGA) functional was used.

The adsorption of DBDS (see Fig. 1) on Cu(111) was modeled using a c7 × 7 periodic unit cell, with the aim to study the adsorption of an isolated adsorbate molecule interacting with the surface. The Cu slab contains three layers, from which the bottom one was not allowed to relax and kept at the bulk positions. The lattice parameter was initially fixed at the experimental value, 3.61 Å, to build the initial slab [52]. Then, it was re-optimized, and a subestimation of 3 % from the original supercell was obtained. This small change is accepted because it is in good agreement with the experimental parameter and obtained theoretically from PBE [53].

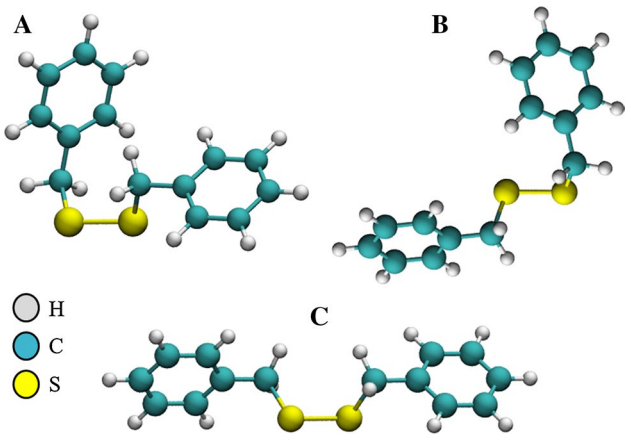

Fig. 1 Three DBDS conformers of the lowest energy used in this study as starting structure to generate the adsorption complex

The sampling in the Brillouin zone was performed employing 4 and 13 k-points, resolved on 2 × 2 × 1 and 5 × 5 × 1 grids for the geometry optimizations (including dispersion corrections) and energy evaluation (at single PBE level), respectively.

Since our system involved organic molecules interacting through weak forces, the pure DFT energies obtained in periodic DFT PBE should be corrected. Therefore, we included Grimme D2 corrections [54], which can be calculated using the presently used VASP version, although D2 corrections overestimate the binding energy ([55, 56] and references therein).

The optimization procedure consisted of locating initially the DBDS molecule at 2.3 Å from the surface, at the beginning of the geometry relaxation. This distance was taken from chemi- and physisorption data reported in several studies involving the adsorption of sulfur molecules on copper surfaces [34, 35, 57, 58].

2.2 Calculation of the adsorption energy and charge transfer

Each complex can be characterized by its adsorption energy, ΔE_{ads}, which is calculated from the total energy of the ground-state optimized geometries of the complex, Cu(111) slab and DBDS as follows:

$$\Delta E_{ads} = E_{Cu(111)-DBDS} - \left[E_{Cu(111)} + E_{(DBDS)}\right] \quad (1)$$

$$\Delta E_{ads.D2} = \Delta E_{ads} + \left[E_{Cu(111)-DBDS.D2} - \left[E_{Cu(111).D2} + E_{(DBDS).D2}\right]\right] \quad (2)$$

Equation (2) includes the dispersion contribution D2, explicitly for each term.

However, this term can be scaled to obtain a better energetic estimation, avoiding the most part of the overestimation of empirical of the metal bulk. A commonly used correction is that the adsorption energy is approximated to include only the dispersion from the top layer of the surface and the adsorbate (DBDS), defining the term $\Delta E_{ads.D2.1layer}$ as:

$$\Delta E_{ads.D2.1layer} = \Delta E_{ads} + \left[\frac{1}{3}\left(E_{Cu(111)-DBDS.D2}\right) - \left[\frac{1}{3}E_{Cu(111).D2} + E_{(DBDS).D2}\right]\right] \quad (3)$$

Moreover, an energetic decomposition scheme can be inspected, to describe energetically the change along the adsorption process, through a two-part scheme of deformation/interaction [59]. This partition scheme consists of two contributions, deformation (ΔE_{def}) and interaction energy (ΔE_{int}), related as:

$$\Delta E_{\text{ads}} = \Delta E_{\text{def}} + \Delta E_{\text{int}} \tag{4}$$

where

$$\Delta E_{\text{def}}(X) = E(X_{\text{deformed}}) - E\left(X_{\text{equilibrium}}\right)$$
$$X = \text{Cu}_{(111)}, \text{DBDS} \tag{5}$$

in which ΔE_{def} represents an energetic measure of perturbation over the gas-phase equilibrium geometry of each molecule, to obtain their respective geometry in the complex. It is clear that ΔE_{int} represents the interaction energy between the deformed molecules in the complex and can be easily computed, from Eqs. (4) and (5).

The amount of total electronic charge transferred between DBDS and the Cu surface was quantified by a global charge transfer descriptor (*GCT*), which corresponds to the sum of atomic charges (q_A) on each molecule (A), i.e., the DBDS or the surface:

$$\text{GCT} = \sum_{A} q_A; \quad A \in Cu_{\text{surf}} \text{ or } \text{DBDS} \tag{6}$$

For this purpose, the Bader Charge Analysis [60, 61] was used.

Additionally, the electron localization function (ELF) was studied to characterize the existence of the S–S bond, while the DBDS interacts with the surface. The ELF of Becke and Edgecombe [62] provides an orbital-independent description of the electron localization based on strong physical arguments regarding the Fermi hole. The ELF is defined in terms of the excess of local kinetic energy density due to the Pauli exclusion principle and the Thomas–Fermi kinetic energy density. Its numerical values are conveniently mapped on the interval (0, 1), facilitating its analysis. According to the interpretation of the ELF, a region of the space with a high value of ELF corresponds to a region where it is more probable to localize a pair of electrons of opposite spin. The topological analysis of the ELF gradient field [63–65] provides a mathematical model enabling the partition of the molecular position space in a set of continuous and non-overlapping basins of attractors that present in principle a one-to-one correspondence with electron pairs.

In this way, an accurate calculation of chemical local objects such as bonds, lone pairs or atomic shells can be achieved. The basins are either core basins labeled C(A) or valence basins V(A,…) belonging to the outermost shell. Valence basins are characterized by their coordination number (synaptic order) with core [66]. The original work of Silvi and Savin on the ELF generated a fruitful field of applications in a variety of chemical problems, ranging from structural and chemical reactivity studies as well as the study of chemical reactions [67–70]. This scheme will be applied to evaluate the S–S bond in the complex.

3 Results and discussion

3.1 Geometric and energetic aspects

In this work, 20 optimized adsorption complexes were defined combining the different possible S adsorption sites on Cu(111) surface (top, hollow hcp, hollow fcc and bridge) with the three isoenergetic DBDS gas-phase conformations, obtained from a previous study [71] (see Fig. 1).

Using PBE, the structure B was more stable than A and C conformers by 0.03 and 0.07 eV, respectively. It confirms the isoenergetic character of three conformers. In the succeeding optimization procedures, the adsorption complexes between DBDS and Cu(111) result with different interaction sites, mainly noticed by S–Cu geometrical parameters. A schematic representation of showing selected geometrical parameters is presented in Fig. 2.

Typically, the adsorption site for both S atoms is found close to a bridge site. Other adsorption sites slightly higher in energy are also present, such as on top (close). Different adsorption geometries (mainly due to different benzyl conformations) showing different adsorption energies can adsorb on the same adsorption site. In order to rationalize the data, we defined the vertical spacing distance Δz and the shortest S–Cu distance, $d1$ and $d2$ (see Fig. 2; Table 1).

The most stable physisorbed geometries, shown in Fig. 3, can be divided into two groups: (a) having an S–Cu atop adsorption and (b) 2S–Cu atop adsorption. The first is slightly more favorable (structure B7). It should be noted that the benzyl groups tend to orient parallel to the Cu(111) surface.

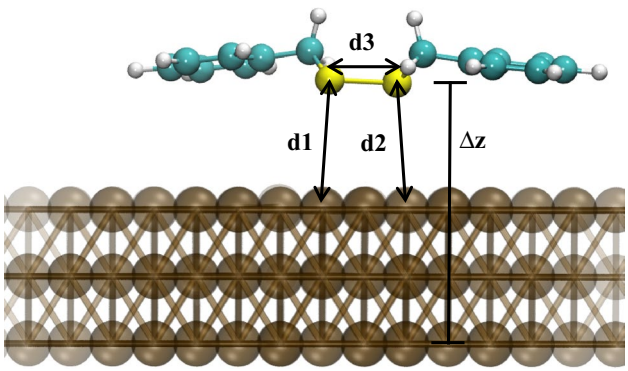

Fig. 2 Schematic representation of the adsorption complex showing selected geometrical parameters used in the discussion of the adsorption site and geometry

Table 1 Geometrical parameters describing the final adsorption geometries and sites: $d1$, $d2$, $d3$ and Δz (for sulfur 1 and sulfur 2, see Fig. 2)

Complex	Final adsorption site (S1, S2)		$d1$	$d2$	$d3$	$\Delta z1$	$\Delta z2$
A1	Bridge-top	Bridge-top	2.75	2.98	2.09	6.47	6.29
A2	Bridge-top	Bridge-top	2.78	2.66	2.09	6.19	6.28
A3	Top	Top	2.96	2.99	2.09	6.48	6.39
A4	Bridge-top	Bridge-top	2.97	3.02	2.09	6.51	6.42
A5	Hollow1-top	Bridge-top	2.57	2.87	2.11	6.51	6.13
A6	Hollow1-top	Bridge-top	2.56	2.95	2.14	6.48	6.07
A7	Bridge-top	Bridge	2.87	3.06	2.08	6.71	6.42
B1	Hollow1-bridge	Hollow1-bridge	2.41	2.42	4.42	5.98	5.96
B2	Hollow1-bridge	Hollow1	2.49	2.31	3.42	5.81	6.03
B3	Hollow1-top	Hollow2	2.81	2.24	3.92	5.67	6.30
B4	Top	Bridge-top	2.93	2.85	2.09	6.38	6.37
B5	Bridge-top	Bridge-top	2.66	2.70	2.13	6.24	6.18
B6	Top	Top	3.00	3.04	2.08	6.58	6.36
B7	Top	Bridge-top	2.82	2.95	2.10	6.40	6.30
B8	Hollow2-top	Hollow1-top	3.02	2.92	2.07	6.58	6.69
C1	Top	Top	2.96	2.97	2.10	6.37	6.46
C2	Hollow2-bridge	Hollow1-bridge	2.58	2.61	2.18	6.14	6.09
C3	Top	Bridge-top	2.95	2.76	2.09	6.29	6.43
C4	Hollow1-top	Hollow2-top	2.77	2.77	2.15	6.40	6.42
C5	Hollow2-top	Hollow1	3.00	3.05	2.07	6.76	6.65

Values in Å

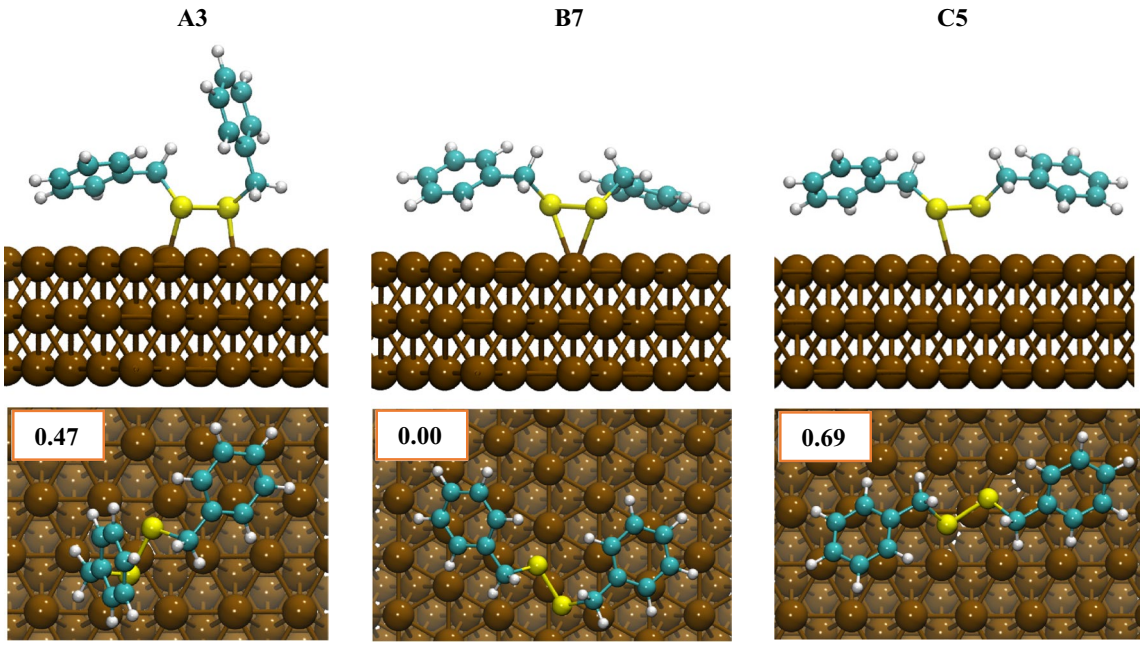

Fig. 3 Some selected structures of physisorbed DBDS on Cu(111), showing their relative adsorption energy (PBE-D2 energies in eV). *In case of D2-1 layer energies, the relative energies are 0.07, 0.00 and 0.25 eV, respectively

From Table 1, the S–S distances ($d3$) between 2.0 and 2.2 Å correspond to physisorbed complexes and also correlate with a high average values of $d1$ and $d2$ (>2.56 Å), with adsorption sites that vary between bridge, top and hollow sites. In the other side, the group of structures having $d3$ distance larger than 3.4 Å and an average of $d1$ and $d2$

lower than 2.56 describes the chemisorption complexes, where sulfur atom prefers the adsorption on bridge (slightly to hollow) sites.

In summary, the most favorable adsorption sites were found to be bi-coordinated bridge in the case of physisorption and a bridge (slightly to hollow) for each dissociated fragment of benzylthiol, in the case of chemisorption (see Figs. 3, 5).

The Δz distance is related to the strength of the interaction of the sulfur atom with the Cu(111) surface. Moreover, the difference of the vertical spacing between the S atom and the closest Cu surface atom and Δz give a geometrical measure for the deformation of the surface. After adsorption, and especially with dissociative chemisorption, a Cu atom can be lifted up out of the surface and can be considered as a precursor state to the formation of an adatom. Similar results have been reported in the adsorption of thiols on Au and Ag surfaces, being less evident than Cu, attributable to the metal hardness. Looking at Δz in Table 1, one can conclude that the effect of chemisorption on the z coordinate of the surface copper atoms is particularly noticeable over $\Delta z1$, where values of $\Delta z1$ lower than 5.98 correspond to chemisorbed species, while higher than this value are related to physisorption complexes. The most affected copper atoms of the top layer are lifted up by 0.2 Å. The magnitude of surface deformation due to the tension generated by the adsorption of DBDS will certainly increase with increasing coverage, as is noticed in thiol/Au(111) SAMs [9, 72]. This surface tension is observed over a range of copper atoms in the neighborhood of the binding sulfur atom (see Fig. 4).

The adsorption energies (see Table 2) are in agreement with the geometrical parameters. Indeed, the adsorption complexes having the shortest distances between the DBDS sulfur atom and the Cu(111) surface ($d1$, $d2$) correlate with the highest (absolute value) adsorption energies. The adsorption energy helps to identify that the phenyl-Cu proximity shows a weak π–Cu interaction (see lower), leading to an extra stabilization of the adsorption complexes (structures B1, B2 and B3), which correspond to the chemisorbed species (see Fig. 5).

In general, the complexes formed from conformer types B and C (see Fig. 1) have more stable adsorption energies due to the proximity of the phenyl groups to the surface, favoring π–Cu interactions.

The deformation/interaction decomposition scheme displayed in Table 3 shows that in case of physisorbed complexes, the surface is slightly more perturbed than DBDS. The low values of ΔE_{def} and almost the total contribution of ΔE_{int} to ΔE_{ads} explain the low geometrical effect in the adsorption. In the other side for chemisorbed complexes, the ΔE_{def} is

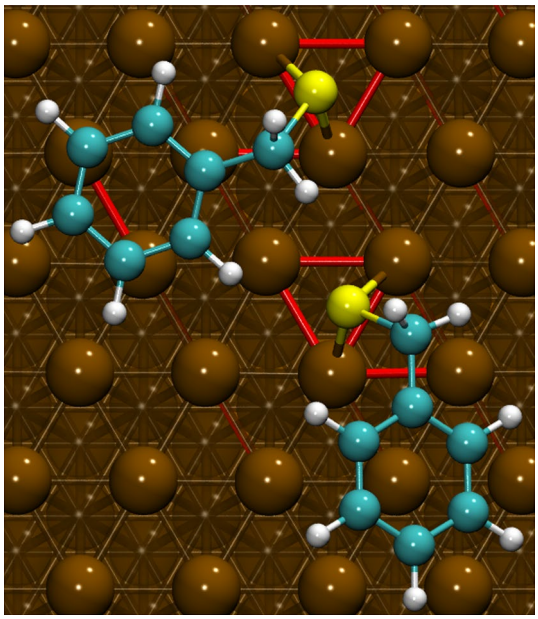

Fig. 4 Adsorption geometry of the most stable dissociated DBDS molecule on Cu(111) showing the distortion through Cu–Cu distances (*in red*) after adsorption

Table 2 Adsorption energy (ΔE_{ads}) and sum of charges (q) on the Cu(111) surface and disulfide S–S atoms in the complexes investigated

Complex	$\Delta E_{ads.D2.all}$	$\Delta E_{ads.PBE}$	$\Delta E_{ads.D2.1layer}$	$q_{Cu(111)}$	$q_{(S–S)}$
A1	−2.09	−0.40	−0.54	−0.14	0.02
A2	−2.03	−0.19	−0.38	−0.10	−0.04
A3	−2.03	−0.52	−0.60	−0.17	0.02
A4	−2.01	−0.58	−0.63	−0.14	0.01
A5	−1.94	−0.25	−0.39	−0.10	−0.02
A6	−1.87	−0.26	−0.38	−0.08	−0.06
A7	−1.54	−0.22	−0.23	−0.11	−0.02
B1	−3.84	−1.18	−1.67	0.67	−0.76
B2	−3.76	−1.01	−1.53	0.67	−0.77
B3	−3.48	−1.03	−1.45	0.62	−0.72
B4	−2.57	−0.21	−0.60	−0.08	−0.05
B5	−2.52	0.07	−0.40	0.01	−0.13
B6	−2.51	0.12	−0.36	−0.09	−0.06
B7	−2.50	−0.14	−0.53	−0.09	−0.05
B8	−1.89	0.10	−0.16	−0.08	−0.05
C1	−2.76	0.17	−0.43	−0.12	0.02
C2	−2.52	0.18	−0.34	0.05	−0.16
C3	−2.34	−0.23	−0.55	−0.10	0.00
C4	−1.98	−0.12	−0.36	−0.03	−0.07
C5	−1.82	−0.09	−0.28	−0.08	−0.02

Values in eV, charges in e

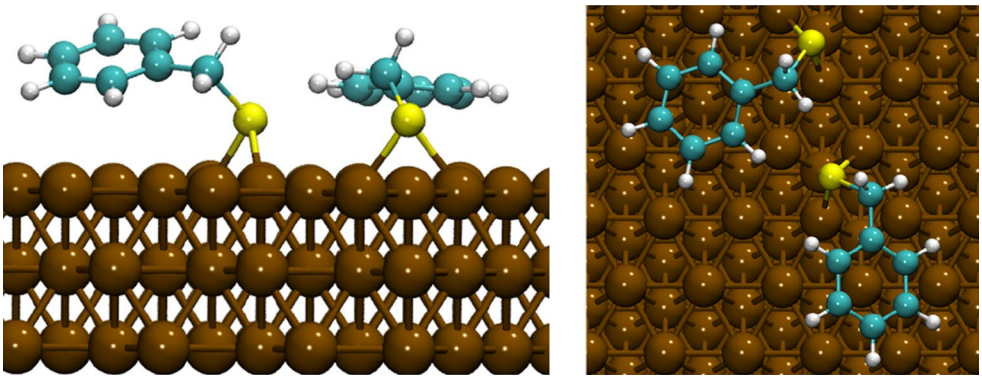

Fig. 5 *Top* and *side* views of the most favorable adsorption geometry (B1) for DBDS on Cu(111)

Table 3 Deformation energies (ΔE_{def}) of surface and DBDS, and interaction energies (ΔE_{int}) for complexes, in the presence and absence of D2 vdW contribution (in eV)

Complex	ΔE_{def} (Cu)	ΔE_{def} (DBDS)	ΔE_{def} (Cu + DBDS)	ΔE_{intD2}	ΔE_{int}
A1	0.15	0.07	0.22	−2.31	−0.66
A2	0.15	0.06	0.21	−2.24	−0.50
A3	0.11	0.11	0.22	−2.25	−0.67
A4	0.15	0.02	0.17	−2.19	−0.69
A5	0.17	0.11	0.28	−2.22	−0.57
A6	0.18	0.09	0.27	−2.15	−0.56
A7	0.14	0.04	0.18	−1.72	−0.36
B1	0.21	3.64	3.85	−7.69	−5.02
B2	0.28	3.13	3.41	−7.17	−4.39
B3	0.35	3.45	3.80	−7.28	−4.68
B4	0.15	0.20	0.35	−2.92	−0.48
B5	0.18	0.27	0.45	−2.97	−0.29
B6	0.17	0.26	0.43	−2.94	−0.24
B7	0.14	0.18	0.33	−2.82	−0.40
B8	0.08	0.10	0.18	−2.07	−0.03
C1	0.15	0.31	0.46	−3.21	−0.32
C2	0.17	0.31	0.48	−3.00	−0.33
C3	0.14	0.16	0.30	−2.63	−0.52
C4	0.20	0.09	0.29	−2.27	−0.34
C5	0.08	0.04	0.12	−1.95	−0.18

Chemisorption complexes are highlighted

higher and particularly ΔE_{def} (DBDS) is greater than the surface, and it represents more than 70 % of ΔE_{ads} with the inclusion of an important part of the dissociative process. Additionally, ΔE_{def} (DBDS) represents more than the 50 % of absolute value of ΔE_{int}, while the ΔE_{def} (Cu) is <5 % for ΔE_{int}. Those assesses explain an important role of the geometry relaxation of DBDS related to dissociation over the adsorption.

3.2 Electronic aspects

3.2.1 Global charge transfer

A global charge transfer descriptor was introduced to quantify the relation between the adsorption energies and charge transfer between DBDS and the Cu(111) surface. Table 2 summarizes this quantity. It can be seen that the direction of the charge transfer is highly related to the kind of adsorption (physi- or chemisorption). In the most stable cases (B1, B2 and B3, i.e., chemisorbed species), the DBDS molecule acts as an electron acceptor. Most transferred charge is then allocated on the disulfide group, reaching a maximum when dissociation of the S–S bond occurs. Conversely, in the physisorption processes, the DBDS molecule acts as donor but with a lower rate of charge transfer to the Cu(111) surface (see Fig. 6).

Also, a spontaneous (barrier less) dissociation of the disulfide bond is observed for chemisorbed species, which increases the ability of DBDS to become an electron acceptor. In this case, the S–S distance increases from 2.0 to 2.2 Å and from 3.5 to 4.5 Å for physisorption and chemisorption, respectively. Finally, bi-coordinated interactions of the sulfur

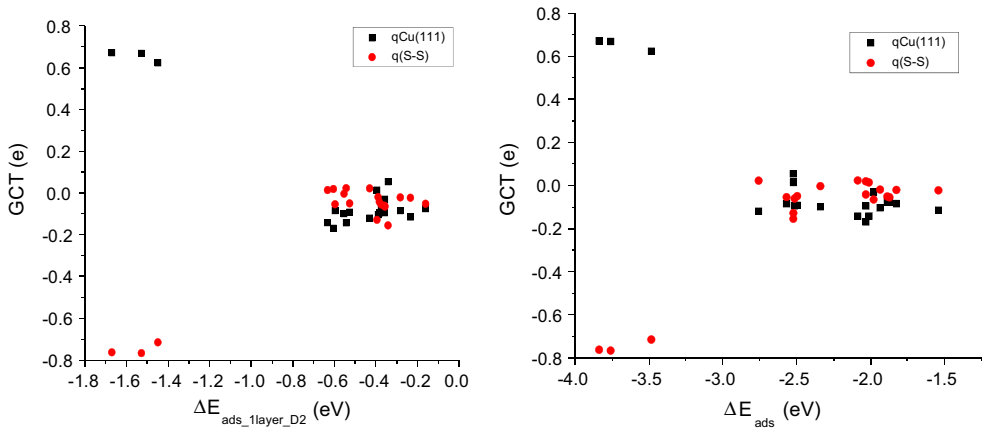

Fig. 6 General charge transfer (GCT) versus adsorption energies ($\Delta E_{\text{ads and}}$ $\Delta E_{\text{ads\_1layer\_D2}}$)

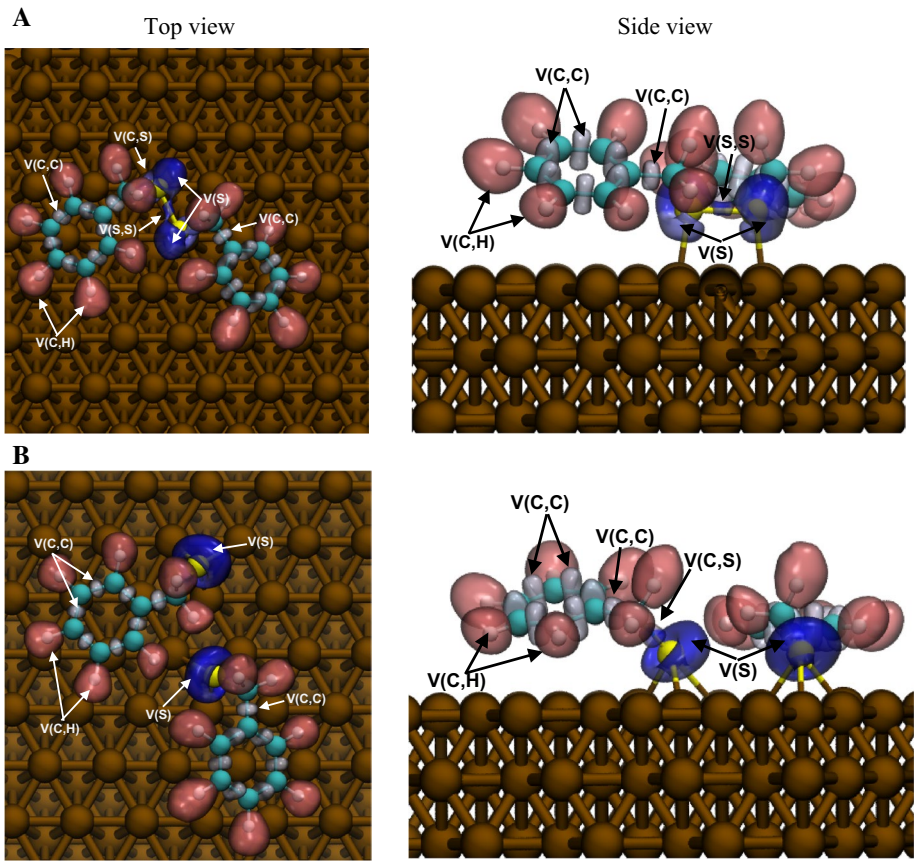

Fig. 7 Selected ELF isosurfaces (ELF = 0.80) for **a** physi- and **b** chemisorption complexes formed by DBDS adsorption on copper surface

atoms with the Cu atoms and preferential orientation of the phenyl rings parallel to the copper surface were observed.

3.2.2 Electron localization function (ELF) analysis

In Fig. 7, a representation of the ELF basins is shown to help visualize the most relevant regions of valence electron density that characterize the DBDS in its adsorption process on copper surface.

The basin population analysis using pseudopotentials is not accurate enough, mainly to describe the population associated with sulfur atoms. However, the topological description gives us important information about the bonds in the different obtained complexes in this work.

In all kinds of formed complexes by physi- or chemisorption, each benzyl sulfide moiety of the adsorbed DBDS presents two kinds of C–H bonds, aromatic (6) and methylene (2), represented by disynaptic basins V(H,C). The six carbon–carbon aromatic bonds are represented by disynaptic V(C–C), the shape and the population, close to 3e, is characteristic for delocalized bonds in aromatic systems, and the one non-aromatic bond, V(C–C), has population close to 2.1 e. Around the sulfur atom is possible to visualize the disynaptic V(C–S) with population between 1 and 1.5e and two monosynaptic basins V(S) which characterize the electron lone pairs. At least one of these is located between sulfur and surface. But the main difference is centered in the disynaptic basin V(S–S), which describes the disulfide bond. In the physisorption complexes it is possible to visualize this basin, however in the chemisorption complexes the V(S-S) disynaptic basin disappears. It indicates the disulfide dissociation in the most stable formed complexes.

Corroboration of the topological description was made using the structure of isolated DBDS, with the geometry adopted in the complex. Initially, the level of calculation previously described was used and the topological description was confirmed by the all electron PBE/def2-TZVP level of calculation. The same description was obtained, and the disynaptic V(S–S) appears and disappears in the DBDS physi- and chemisorption complexes, respectively.

4 Conclusions

The molecular (physisorption) and dissociative (chemisorption) adsorption of DBDS on Cu(111) was studied by means of periodic DFT. Physisorption was investigated in detail by optimizing systematically all possible conformations. The adsorption site was found to be bi-coordinated bridge for physisorption and on simple bridge for chemisorption. The adsorption energies were calculated and decomposed, validating the high contribution of relaxation in the adsorption process. The charge transfer and the ELF function were used to describe the electronic structure of the adsorption complex. It was found that a charge transfer from the Cu(111) surface to the disulfide group occurs, reaching a maximum in the structures where S–S bond dissociation is observed, whereas in the physisorption processes, the DBDS molecule acts as donor but with a lower rate of charge transfer to the Cu surface. The ELF shows the absence and presence of the S–S bond in chemisorption and physisorption, respectively.

The dissociative adsorption of DBDS on Cu(111) can be considered as the first step of the copper corrosion phenomenon in which an oxidation process takes place on the surface.

Acknowledgments The authors acknowledge the financial support by FONDECYT through the Project Number 1120785 and Universidad Andres Bello Grant DI-497-14/R. M.S.-T. thanks CONICYT for a Ph.D. scholarship and Universidad Andres Bello for support through grant DI40/12-I. F.T. thanks FONDECYT for several appointments as Invited Professor (2013 and 2015).

References

1. Ulman A (1996) Chem Rev 96:1533–1554
2. Love JC, Estroff LA, Kriebel JK, Nuzzo RG, Whitesides GM (2005) Chem Rev 105:1103–1169
3. Vericat C, Vela ME, Benitez G, Carro P, Salvarezza RC (2010) Chem Soc Rev 39:1805–1834
4. Cometto FP, Paredes-Olivera P, Macagno VA, Patrito EM (2005) J Phys Chem B 109:21737–21748
5. Gronbeck H (2010) J Phys Chem C 114:15973–15978
6. Laibinis PE, Whitesides GM, Allara DL, Tao YT, Parikh AN, Nuzzo RG (1991) J Am Chem Soc 113:7152–7167
7. Kacprzak KA, Lopez-Acevedo O, Hakkinen H, Gronbeck H (2010) J Phys Chem C 114:13571–13576
8. Fonticelli MH, Benitez G, Carro P, Azzaroni O, Salvarezza RC, Gonzalez S, Torres D, Illas F (2008) J Phys Chem C 112:4557–4563
9. Luque NB, Santos E, Andres J, Tielens F (2011) Langmuir 27:14514–14521
10. Sawaguchi T, Sato Y, Mizutani F (2001) J Electroanal Chem 496:50–60
11. Woodruff DP (2007) Appl Surf Sci 254:76–81
12. Woodruff DP (2008) Phys Chem Chem Phys 10:7211–7221
13. Tielens F, Costa D, Humblot V, Pradier CM (2008) J Phys Chem C 112:182–190
14. Tielens F, Santos E (2010) J Phys Chem C 114:9444–9452
15. Doneux T, Tielens F, Geerlings P, Buess-Herman C (2006) J Phys Chem A 110:11346–11352
16. Andreoni W, Curioni A, Gronbeck H (2000) Int J Quantum Chem 80:598–608
17. Cometto FP, Macagno VA, Paredes-Olivera P, Patrito EM, Ascolani H, Zampieri G (2010) J Phys Chem C 114:10183–10194
18. Di Felice R, Selloni A (2004) J Chem Phys 120:4906–4914
19. Gronbeck H, Curioni A, Andreoni W (2000) J Am Chem Soc 122:3839–3842
20. Humblot V, Tielens F, Luque NB, Hampartsoumian H, Methivier C, Pradier C-M (2014) Langmuir 30:203–212
21. Naitabdi A, Humblot V (2010) Appl Phys Lett 97:223112
22. Méthivier C, Humblot V, Pradier C-M (2015) Surf Sci 632:88–92
23. Schiffrin A, Riemann A, Auwarter W, Pennec Y, Weber-Bargioni A, Cvetko D, Cossaro A, Morgante A, Barth JV (2007) Proc Natl Acad Sci USA 104:5279–5284
24. Schiffrin A, Reichert J, Pennec Y, Auwaerter W, Weber-Bargioni A, Marschall M, Dell'Angela M, Cvetko D, Bavdek G, Cossaro A, Morgante A, Barth JV (2009) J Phys Chem C 113:12101–12108
25. De Renzi V, Lavagnino L, Corradini V, Biagi R, Canepa M, del Pennino U (2008) J Phys Chem C 112:14439–14445
26. Di Felice R, Selloni A, Molinari E (2003) J Phys Chem B 107:1151–1156
27. Gonella G, Terreni S, Cvetko D, Cossaro A, Mattera L, Cavalleri O, Rolandi R, Morgante A, Floreano L, Canepa M (2005) J Phys Chem B 109:18003–18009
28. Hoffling B, Ortmann F, Hannewald K, Bechstedt F (2010) Adsorption of cysteine on the Au(110)-surface: a density functional theory study. Springer, Berlin

29. Fischer S, Papageorgiou AC, Marschall M, Reichert J, Diller K, Klappenberger F, Allegretti F, Nefedov A, Woell C, Barth JV (2012) J Phys Chem C 116:20356–20362
30. Luque NB, Santos E (2012) Langmuir 28:11472–11480
31. Santos E, Avalle L, Poetting K, Velez P, Jones H (2008) Electrochim Acta 53:6807–6817
32. Santos E, Avalle LB, Scurtu R, Jones H (2007) Chem Phys 342:236–244
33. Marti EM, Methivier C, Pradier CM (2004) Langmuir 20:10223–10230
34. Rieley H, Kendall GK, Chan A, Jones RG, Ludecke J, Woodruff DP, Cowie BCC (1997) Surf Sci 392:143–152
35. Fan X-L, Liu Y, Ran R-X, Lau W-M (2013) J Phys Chem C 117:6587–6593
36. Barlow SM, Raval R (2003) Surf Sci Rep 50:201–341
37. Tumiatti V, Maina R, Scatiggio , Pompili M, Bartnikas R (2008) In: Conference Record of the 2008 IEEE International Symposium on Electrical Insulation, pp 284–286
38. Lukic JM, Milosavljevic SB, Orlovic AM (2010) Ind Eng Chem Res 49:9600–9608
39. Toyama S, Tanimura J, Yamada N, Nagao E, Amimoto T (2009) IEEE Trans Dielectr Electr Insul 16:509–515
40. Ahmed Khan F, Sundara Rajan J, Ansari MZA, Asra PS (2012) In: 2012 International Conference on Advances in Power Conversion and Energy Technologies (APCET), pp 1–4
41. Oweimreen GA, Jaber AMY, Abulkibash AM, Mehanna NA (2012) IEEE Trans Dielectr Electr Insul 19:1962–1970
42. Maina R, Tumiatti V, Pompili M, Bartnikas R (2009) IEEE Trans Dielectr Electr Insul 16:1655–1663
43. Tielens F, Humblot V, Pradier C-M (2008) Int J Quantum Chem 108:1792–1795
44. Tielens F, Humblot V, Pradier CM, Calatayud M, Illas F (2009) Langmuir 25:9980–9985
45. Tielens F, Santos E (2010) J Phys Chem C 114:9444–9452
46. Kresse G, Hafner J (1993) Phys Rev B 47:558–561
47. Kresse G, Hafner J (1994) Phys Rev B 49:14251–14269
48. Blochl PE (1994) Phys Rev B 50:17953–17979
49. Kresse G, Joubert D (1999) Phys Rev B 59:1758–1775
50. Hammer B, Hansen LB, Norskov JK (1999) Phys Rev B 59:7413–7421
51. Perdew JP, Burke K, Ernzerhof M (1997) Phys Rev Lett 78:1396–1396
52. Straumanis ME, Yu LS (1969) Acta Crystallogr Sect A 25:676–682
53. Gattinoni C, Michaelides A (2015) Faraday Discuss 180:439–458
54. Grimme S (2006) J Comput Chem 27:1787–1799
55. Almora-Barrios N, Carchini G, Blonski P, Lopez N (2014) J Chem Theory Comput 10:5002–5009
56. Klimes J, Michaelides A (2012) J Chem Phys 137:120901
57. Ferral A, Patrito EM, Paredes-Olivera P (2006) J Phys Chem B 110:17050–17062
58. Crutcher ER, Warner K, Northwest M, electric-connectionco.com
59. Scaranto J, Mallia G, Harrison NM (2011) Comput Mater Sci 50:2080–2086
60. Henkelman G, Arnaldsson A, Jónsson H (2006) Comput Mater Sci 36:354–360
61. Tang W, Sanville E, Henkelman G (2009) J Phys: Condens Matter 21:084204
62. Becke AD, Edgecombe KE (1990) J Chem Phys 92:5397
63. Savin A, Becke AD, Flad J, Nesper R, Preuss H, von Schnering HG (1991) Angew Chem Int Ed Engl 30:409–412
64. Savin A, Jepsen O, Flad J, Andersen OK, Preuss H, von Schnering HG (1992) Angew Chem Int Ed Engl 31:187–188
65. Silvi B, Savin A (1994) Nature 371:683–686
66. Silvi B (2002) J Mol Struct 614:3–10
67. Melin J, Fuentealba P (2003) Int J Quantum Chem 92:381–390
68. Fuentealba P, Chamorro E, Santos JC (2007) In: Toro-Labbe A (ed) Theoretical aspects of chemical reactivity, vol 19, pp 57–85
69. Santos JC, Andres J, Aizman A, Fuentealba P, Polo V (2005) J Phys Chem A 109:3687–3693
70. Santos JC, Tiznado W, Contreras R, Fuentealba P (2004) J Chem Phys 120:1670–1673
71. Saavedra-Torres M, Jaque P, Tielens F, Santos JC (2015) Theoret Chem Acc 134:73
72. Bedford E, Humblot V, Méthivier C, Pradier CM, Gu F, Tielens F, Boujday S (2015) Chem Eur 21:14555–14561